P1.22 A NEW AUTOMATED METHOD OF MFRSR-BASED OPTICAL DEPTH ANALYSIS

John A. Augustine* and Carlos I. Medina†
NOAA Air Resources Laboratory
Surface Radiation Research Branch (SRRB)
Boulder, Colorado 80305

†Department of Engineering
Colorado School of Mines
Golden, Colorado

1. INTRODUCTION

Modern robotic spectral solar instruments designed for retrievals of aerosol optical depth (AOD), such as the Multi-Filter Rotating Shadowband Radiometer (MFRSR) (Harrison et al. 1994), usually operate in an unattended mode. Thus their raw data sets sample a wide range of atmospheric conditions, most of which are undesirable for aerosol optical depth analysis. In addition, these instruments are often not calibrated for absolute irradiance, and must be calibrated for AOD analysis from their own operational data. For AOD retrievals, this involves extrapolation to the value that the instrument would measure before the sun's beam enters the earth's atmosphere, i.e., the extraterrestrial, or zero air mass signal (I_0). This value is inferred via the Langley method (Shaw 1983). Recently, a method that utilizes component solar measurements (direct and diffuse) to identify totally clear-sky and non-hazy periods (Long and Ackerman 2000) has been used successfully to screen MFRSR data for spectral solar measurements suitable for calibration Langley plots (Augustine et al. 2003). This method was tested in a proof-of-concept mode on a two-month period during the Spring of 2001 with data from the Table Mountain SURFRAD station near Boulder, Colo. The resultant calibration was subsequently applied to an Asian dust event that occurred within that period, and verified with independent aerosol optical depth measurements from a nearby MFRSR and an automated sun photometer.

Although this new method of MFRSR spectral channel calibration is free of any subjective decision making, it has been shown to work for one event and for one station, using a spreadsheet program. Here, we describe how the new method has been improved, fully automated, and applied to successfully different locations.

2. THE SURFRAD NETWORK

The SURFRAD network (Figure 1), has been operating over the United States since 1995 (Augustine et al. 2000). It is the first and only national surface radiation budget network for the United States. Primary measurements at SURFRAD stations are the downwelling and upwelling components of broadband solar and thermal infrared irradiance. Solar component measurements (direct and diffuse), basic meteorological variables, and parameters of special interest, including spectral solar, UVB, and photosynthetically active radiation are also made. SURFRAD stations are located in diverse climatic regions of the U.S. Total Sky Imagers (TSI) were added to SURFRAD stations in 1999. All SURFRAD stations have, or have access to, an MFRSR, which makes spectral solar diffuse and global measurements that may be used to compute aerosol optical depth, as well as other parameters. MFRSR data are downloaded from SURFRAD stations daily along with the surface radiation budget measurements.

3. THE MFRSR

Components of the MFRSR pertinent to this discussion are a horizontal circular aperture covered by a white diffuser disk, and a rotating shadowband that intermittently shades the diffuser. Global measurements are made while the shadowband is at rest outside the diffuser's field of view. Diffuse measurements are made when the band rotates to a position such that it shades the diffuser disk. Thus, the MFRSR

*Corresponding author address: John A. Augustine, NOAA/ARL, Surface Radiation Research Branch, R/ARL, 325 Broadway, Boulder, CO, 80305; e-mail: John.A.Augustine@noaa.gov

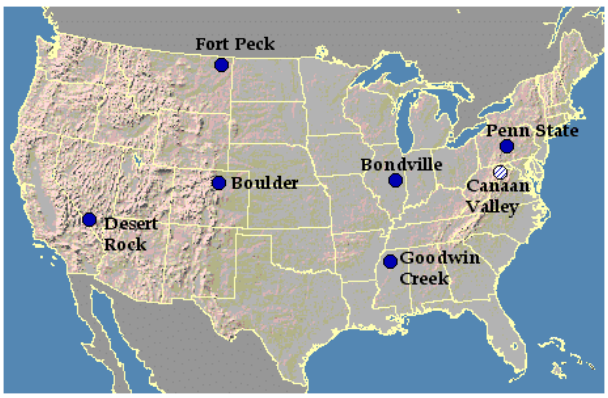

Figure 1. The SURFRAD surface radiation budget network.

alternately measures global and diffuse irradiance impinging on a *horizontal* surface. Accurate positioning of the band is controlled by an ephemeris calculation. This instrument is designed to minimize measurement errors caused by the shadowband. During the band's rotation it stops three times: 1) just before the shadow shades the disk, 2) with its shadow over the diffuser disk, and 3) with its shadow on the other side of the disk. Measurements made with the shadow on either side of the diffuser are used to estimate the fraction of diffuse irradiance blocked by the shadowband when the disk is shaded, which is then added back into the diffuse measurement. The *horizontal* component of the direct beam is inferred by subtracting the corrected diffuse measurement from the global measurement. The direct component at *normal* incidence to the sun is computed by dividing horizontal component of the direct beam by the cosine of the solar zenith angle, which is accurately provided by the ephemeris calculation. In this way, an MFRSR mimics direct normal measurements of a sun photometer. Radiation that passes through the diffuser disk is received simultaneously by seven silicon sensors: a total solar channel and six spectral channels that measure irradiance in 10-nm-wide bands ranging from the ultraviolet to the near infrared, peaking nominally at 415, 500, 615, 670, 870, and 940 nm. In processing MFRSR data, measured signals are corrected for the cosine error of the instrument as documented by the manufacturer, however, these characteristics may change as the instrument ages.

MFRSRs at SURFRAD stations are programmed to sample at 15-second intervals and to provide two-minute averages. Data accessed from cooperating MFRSR networks collocated with SURFRAD stations have different averaging periods, e.g., that from the USDA UV network have three minute temporal resolution, but this incongruity is handled by software that matches the clear-sky and MFRSR data.

4. METHOD

The Langley plot, a graphical form of Beer's Law, is made by plotting the natural log of direct-normal monochromatic spectral measurements versus the optical path length of the sun's beam through the atmosphere for various times of day. The *total optical depth* of the atmosphere for a particular wavelength is contained in the slope of a Langley plot. *Aerosol optical depth* may be extracted from the total by subtracting out contributions from all scattering and absorbing sources other than aerosols. Several factors increase the uncertainty of a single Langley plot's slope, e. g., a change in aerosol concentrations over the course of the day, effects of atmospheric noise such as that from sub-visual cirrus (Shaw 1976), and instrument errors. Also, Harrison et al. (1994) report that the relatively large field of view of an MFRSR makes it vulnerable to the adverse effects of enhanced forward scattering by aerosols or thin cirrus cloud particles whose dimensions are large compared to the wavelength of the measurement. These artificially enhanced signals erroneously decrease the inferred total optical depth. Problems such as these suggest that a single Langley plot for a particular morning or afternoon may not provide accurate AOD information.

It is best to establish a mean calibration I_0 (the zero air mass y-intercept of a Langley plot) that is representative of a several week period surrounding a particular event for which an AOD analysis is desired. Its value represents the measurement the instrument would make at the top of the atmosphere. Once established, it can serve as the instrument's calibration for optical depth analysis for the calibration period. However, periodic re-definition of I_0 for a particular instrument throughout the year is necessary because the extraterrestrial signal will slowly change owing to filter drift and periodic changes in the earth-sun distance. To reduce uncertainty when computing I_0, only times of good air quality and unobscured views of the solar disk should be used. This procedure is common. For example Michalsky et al. (2001) use the 20 most linear Langley plots over a six-week period, which were further pared to ten using an objective method reported by Forgan (1988). Other methods of Langley plot calibration have been reported, e. g.,

Shaw (1976) and Reagan et al. (1984), but most involve a manual selection of calibration data representing the clearest skies and radiatively stable conditions.

Harrison and Michalsky (1994) state that "The simple minded notion of using a least squares regression on all [MFRSR] data works only under true clear-sky conditions." Here, we apply that principle by screening MFRSR data for calibration Langley plots using the clear-sky detection algorithm of Long and Ackerman (2000) as guidance. The Long and Ackerman algorithm operates on broadband solar component (direct and diffuse) data, and applies empirical means to determine clear-sky periods. Broadband solar component data for this analysis may be provided by an MFRSR's broadband channel or by collocated independent measurements, such as those from a SURFRAD station. However, to apply the clear-sky detection algorithm to MFRSR data alone, its broadband channel must be nominally calibrated for absolute irradiance.

The Long and Ackerman (2000) clear-sky detection algorithm is completely automated; only the period to be processed is specified. To detect cloud-free skies, it employs four sequential tests that scrutinize total solar (direct + diffuse) and diffuse solar irradiance. These tests are based on the premise that cloudy and hazy skies exhibit characteristics in the components of downwelling shortwave irradiance that clear skies do not. The first two tests eliminate periods of obvious cloudiness by comparing normalized transformations of total and diffuse solar measurements to expected clear-sky limits. The other two examine temporal variations of parameters computed from the total and diffuse solar irradiance to eliminate more subtle periods of thin cloud or hazy conditions. While each test alone will not detect every clear-sky period, the net of all four represents a fairly complete screening. Identified clear-sky periods correspond to conditions of cloud-free skies for an effective 160° field of view centered on the zenith. Sample results for a day of SURFRAD data are shown in Figure 2. The points marked by solid dots are times identified as clear.

If a sufficient number of clear periods are detected, the Long and Ackerman method will also empirically fit the locus of total, direct, and diffuse clear-sky measurements to daily envelopes of normally expected clear-sky irradiance for those parameters, e. g., the green and orange curves in Figure 2. Their method also interpolates clear-sky envelopes to days for which such empirical fits are

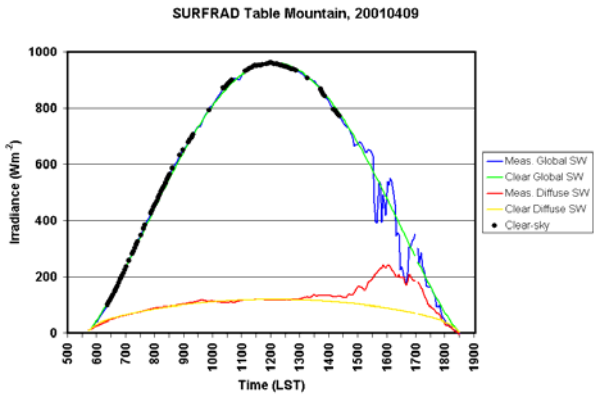

Figure 2. Clear-sky identification results for 9 April 2001 at Table Mountain, Colo. The blue and red curves represent broadband global and diffuse solar measurements. Black dots indicate times determined to be cloud-free. The green and orange curves are empirical daily fits to the clear-sky global and diffuse solar measurements, respectively.

not possible owing to too much cloud. The difference between an irradiance measurement and its corresponding point on the clear-sky envelope for a particular time represents accurate solar forcing owing to clouds or aerosols for that time.

The advantage of using only clear-sky MFRSR data for calibration Langley plots is that noise is reduced and a confident extrapolation to I_0 by simple linear regression is feasible. Figure 3 shows the morning calibration Langley plot produced from the clear-sky periods (black dots) in Figure 2. Note that the clear-sky-screened MFRSR 500-nm measurements (blue dots) form a nearly linear path with little variation. The red line shown is a least squares fit to those points only.

The example in Figure 3 is particularly pristine, i. e., those points not identified as clear (open circles) appear to represent direct measurements that are not obscured by cloud; nor do they appear to be affected by instrument error, or changes in aerosol loading. In other cases, such as that in Figure 4, these types of problems can adversely affect the definition of a representative I_0. Note that the clear-sky analysis successfully screened out the cloudy data on the left side of Figure 4. To reduce the adverse effects of cosine-errors on retrieved AODs in the automated method, only data representing optical path lengths less than 6.0 are considered. Note that the data showing a changing slope (on the right) are not considered. The result of the clear-sky screening and path

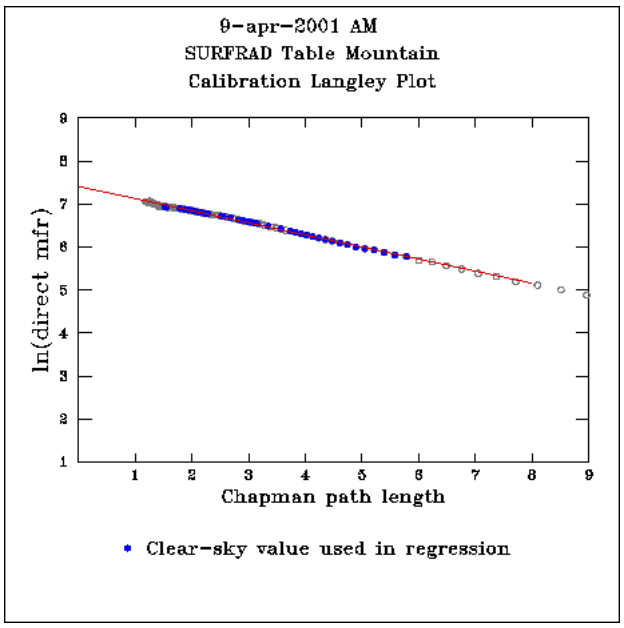

Figure 3. Calibration Langley plot for 9 April 2001. Blue dots represent MFRSR 500 nm measurements that correspond to the clear-sky periods shown in Figure 2.

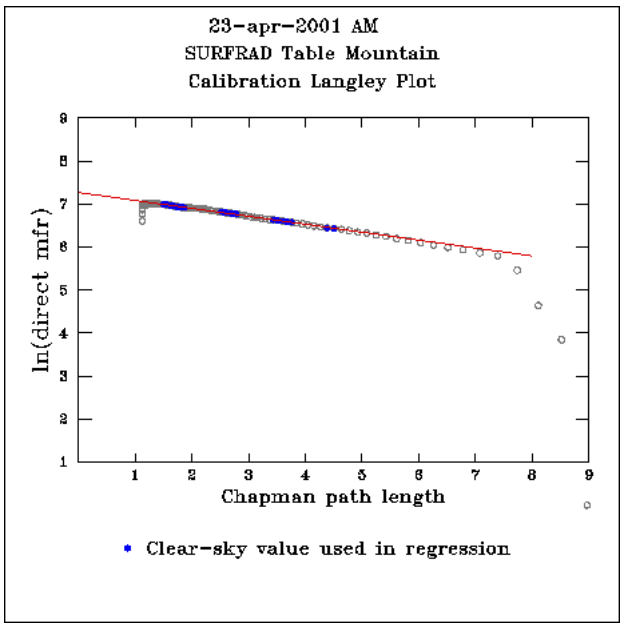

Figure 4. Calibration Langley plot for 23 April 2001. Blue dots represent MFRSR 500 nm measurements that correspond to clear-sky periods identified by the Long and Ackerman clear-sky detection method.

length restrictions is that the clear-sky MFRSR measurements in Figure 4 (blue dots) align nicely in a straight line. Without these, the slope and intercept of the best-fit line of the data in Figure 4 would likely have been different, even if the obvious outliers were disregarded.

Constructing several of these clear-sky Langley plots over a several week period produces a pool of extrapolated I_0 values from which a reliable mean may be computed. The Long and Ackerman clear-sky detection method depends on minimum levels of, and the temporal stability of, diffuse solar irradiance. Therefore, its use to screen MFRSR data for calibration periods increases confidence that the mean, or calibration I_0, will be stable and free of any effects that promote increases in diffuse solar radiation, e. g., high aerosol content or cirrus clouds. After a calibration I_0 is established for a particular wavelength of measurement, it may be applied to any MFRSR measurement at that wavelength within the calibration period, as the anchor point of a two-point Langley plot from which an AOD may be retrieved. Accordingly, application to a series of MFRSR measurements would provide a time series of AOD. According to Harrison et al. (1994), any adverse effects from cirrus clouds or sub-visual cirrus would appear as noise in such a series, and thus would be easily distinguished from the more stable AOD signal. Although 500 nm channel data are utilized here, the calibration method described is applicable to any MFRSR channel.

5. FULL AUTOMATION AND IMPROVEMENT

The method of MFRSR calibration and AOD analysis has been completely automated and improved. It operates on a user-defined period of usually a month or two. First, MFRSR data times are matched to periods of clear sky, as reported by the clear-sky analysis results. The algorithm then splits the clear-sky-screened MFRSR data into morning and afternoon periods, and constructs a set of calibration Langley plots. Next, the algorithm applies linear regression to each clear-sky Langley plot. From those, a pool of I_0 intercepts is assembled, and a mean and standard deviation is computed. I_0 values beyond one standard deviation from the mean are eliminated, and the remaining values are averaged to produce a more accurate calibration I_0 and standard error. This attempt to increase the accuracy of the ultimate I_0 calibration value was alluded to, but not applied in Augustine et al. (2003). The resultant I_0 is applied to individual MFRSR 500-nm measurements within the calibration period to compute the total optical depth. Contributions to the total optical depth from molecular scattering and ozone absorption are removed using methods reported in Augustine et al. (2003). Absorption by

NO_2 is ignored because it was shown in Augustine et al. (2003) to be negligible for 500 nm measurements, even in cases of very high air pollution.

The first test of the completely automated method was to reprocess the period analyzed in Augustine et al. (2003). For that two month period (late March through late May 2001), the automated algorithm chose 15 periods that it deemed suitable for calibration Langley plots, whereas the semi-automated method used in Augustine et al. (2003) used 18. This discrepancy is explained by the practice of the automated method to reject measurements made for optical path lengths less than 1.5 and greater than 6, as recommended by Harrison and Michalsky (1994). This restriction was not applied in Augustine et al. (2003). The mean I_0 computed by the new automated version of 7.387 ±0.023 compares well to the value reported in Augustine et al. (2003) of 7.38 ±0.057, although the standard error was reduced by more than half by the new methodology. This greater accuracy reduced the reported range of AOD error from ±0.01 to ±0.05 (in Augustine et al. 2003) to <±0.01 to ±0.02 (see Figure 5). The weighted averaging that was applied to the 18 calibration I_0 values in Augustine et al. (2003), was not applied in the automated method because, in all cases tested, there was little difference between a normal average and the weighted average.

The fully automated MFRSR calibration code was run for the Bondville MFRSR for the month of October 2001. Bondville was chosen because the SURFRAD station there is collocated with an AERONET sun photometer (Holben et al. 2001). Eight morning and seven afternoon periods during that month were determined to have a suitable number of clear-sky periods for calibration Langley plots. Of the fifteen extrapolated I_0 values, five were rejected because they were more than one standard deviation from the mean. The mean of the remaining 10 values of 0.644 ± 0.021 represents the calibration I_0 for that month. The MFRSR at Bondville is calibrated and thus provides irradiance values. Therefore the I_0 obtained is different in magnitude than that for Table Mountain reported above. However, this difference is inconsequential because it is the slope of the Langley plot that contains the necessary information for an AOD analysis. The computed calibration I_0 was applied to Bondville MFRSR 500-nm data for 3 October 2001. Results are shown in Figure 6. The AOD values are indicated by the open green triangles,

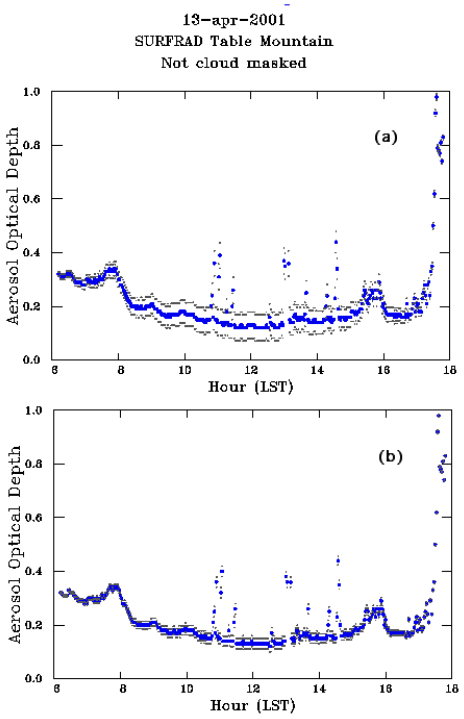

Figure 5. Aerosol optical depth time series for 13 April 2001(blue dots), with (a) error (gray) reported in Augustine et al. (2003), and (b) reduced error using the new more accurate method of I_0 selection.

and the error bounds on the AOD values, computed using the standard deviation of the calibration I_0 sample, are represented by the horizontal bars. Time is presented in UTC to facilitate comparison with AERONET results (Figure 7). The trend in aerosol loading for that day is upward, with the lowest values of about 0.1 occurring in the early morning. The aerosol optical depth ramps up to a short-lived peak of >0.2 around noon (1800 UTC), then appears to settle to a mean value of about 0.17 for remainder of the afternoon, with intermittent spikes of short-lived higher values.

The AOD analysis of the Bondville AERONET sunphotometer 500 channel data in Figure 7 (green curve) shows a nearly identical AOD time series as the MFRSR-based results in Figure 6. Given the similarity of these time series, the random nature of the comparison, and the fact that the MFRSR and AERONET instruments are quite different, offers encouragement that the automated method presented in this paper provides reliable AOD data.

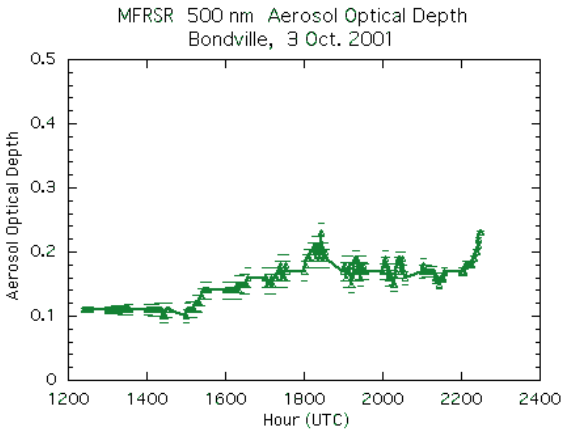

Figure 6. Aerosol optical depth time series at Bondville, Ill. for 3 October 2001 (green triangles), with error indicated by the horizontal lines above and below. These values were derived from MFRSR 500 nm data using the automated algorithm described in this paper.

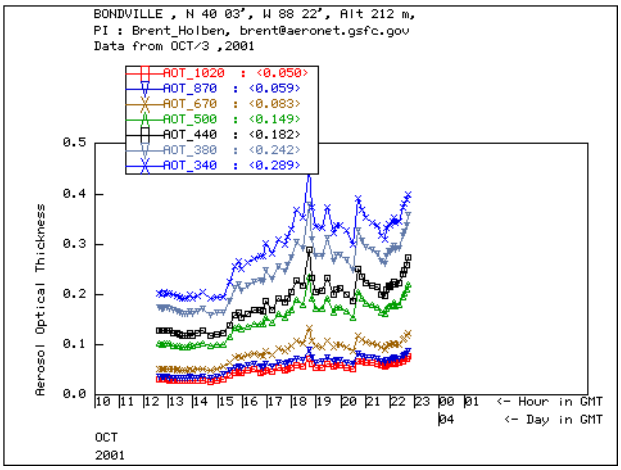

Figure 7. AERONET aerosol optical depth time series for Bondville, Ill. for 3 October 2001. The green triangles are AOD values derived from the 500-nm channel of the AERONET sunphotometer. This plot was obtained from the AERONET web site.

6. SUMMARY AND CONCLUSIONS

A method of MFRSR calibration for aerosol optical depth analysis that uses a clear-sky analysis to screen MFRSR spectral information for suitable calibration data has been developed. A proof-of-concept article (Augustine et al. 2003) showed that the method indeed produces good AOD results. In this paper, the full automation of that method is described. It has been improved, and shown to work successfully in different locations. In summary, the automated algorithm uses a clear-sky analysis of broadband solar component data to select MFRSR spectral data for calibration Langley plots over a period of a month or two. A pool of calibration I_0 values is generated, and a representative mean is computed. The sample is narrowed by eliminating all I_0 values that are more than one standard deviation from the mean. A new mean and standard deviation is computed from the reduced set. This value represents the calibration I_0 and standard error for the calibration period.

The automated method was able to reproduce the results presented in Augustine et al. (2003). It was also randomly applied to SURFRAD data from Bondville, Ill for the month of October 2001. The resultant calibration I_0 value was used to compute a time series of AOD for a day within the calibration period. Results were very similar in phase and magnitude to independent AOD measurements made at a collocated AERONET station. These encouraging results suggest that an operational analysis of AOD at SURFRAD stations is forthcoming. The only remaining task is to develop a reliable cloud-masking feature to eliminate MFRSR measurements that are contaminated by cloud interference before computing a time series of AOD.

7. REFERENCES

Augustine, J. A., C. R. Cornwall, G. B. Hodges, C. N. Long, C. I. Medina, and J. J. DeLuisi, 2003: An automated method for MFRSR calibration and aerosol optical depth analysis with application to an Asian dust outbreak over the United States, *J. Appl. Meteor.*, (in press).

Augustine, J. A., J. J. DeLuisi, and C. N. Long, 2000: SURFRAD—A national surface radiation budget network for atmospheric research, *Bull. Amer. Meteor. Soc.*, **81**, 2341-2357.

Forgan, B. W., 1988: Sun Photometer calibration by the ratio-Langley method. *Baseline Atmospheric Program*, B. W. Forgan and P. J. Fraser, Ed., Bureau of Meteorology, Melbourne, Australia, 22-26.

Harrison, L, J. Michalsky, and J. Berndt, 1994: Automated multifilter rotating shadow-band radiometer: an instrument for optical depth and radiation measurements. *Appl. Opt.*, **33**, 5118-5125.

Harrison, L, and J. Michalsky, 1994: Objective algorithms for the retrieval of optical depths from ground-based measurements. *Appl. Opt.*, **33**, 5126-5132.

Holben, B. N., D. Tanre, A Smirnov, T. F. Eck, I. Slutsker, N. Abuhassan, W. W. Newcomb, J. S. Schafer, B. Chatenet, F. Lavenu, Y. J. Kaufman, J. Vande Castle, A. Setzer, B. Markham, D. Clark, R. Frouin, R. Halthore, A. Karnieli, N. T. O'Neill, C. Pietras, R. T. Pinker, K. Voss, and G. Zibordi, 2001: An emerging ground-based aerosol climatology: Aerosol optical depth from AERONET. *J. Geophys. Res*., **106**, D11, 12067-12097.

Long, C. N., and T. P. Ackerman, 2000: Identification of clear skies from broadband pyranometer measurements and calculation of downwelling shortwave cloud effects. *J. Geophys. Res.*, **105**, No. D12, 15609-15626.

Michalsky, J. J., J. A. Schlemmer, W. E. Berkheiser, J. L. Berndt, and L. C. Harrison, 2001: Multiyear measurements of aerosol optical depth in the Atmospheric Radiation Measurement and Quantitative Links programs. *J. Geophys. Res*., **106**, D11, 12099-12107.

Reagan, J. A., I. C. Scott-Fleming, B. M. Herman, and R. M. Schotland, 1984: Recovery of spectral optical depth and zero airmass solar spectral irradiance under conditions of temporarily varying optical depth. Proceedings*, International Geoscience and Remote Sensing Symposium*, Strasbourg, France, European Space Agency, 455-459.

Shaw, G. E., 1983: Sun photometry. *Bull. Amer. Meteor. Soc.,* **64**, 4-10.

Shaw, G. E., 1976: Error analysis of multi-wavelength sun photometry. *Pure Appl. Geophys*., **114**, 1-14.